

Nonlinear Optical Absorption and Reflection of Single Wall Carbon Nanotube Thin Films by Z-Scan Technique

Daisuke Shimamoto, Takaaki Sakurai, Minoru Itoh, Yoong Ahm Kim*, Takuya Hayashi, Morinobu Endo

Faculty of Engineering, Shinshu University, 4-17-1 Wakasato, Nagano 380-8553, Japan

Mauricio Terrones

Advanced Materials Department, IPICYT, San Luis Potosi 78210, México

Abstract

Both the nonlinear optical transmission and reflection characteristics of HiPco-based single wall carbon nanotube (SWNT) thin films are studied by using the Z-scan method with femtosecond laser pulses at a wavelength of 1.46 μm . The nonlinear absorption coefficient and nonlinear refractive index are obtained as $(5.4 \pm 2.0) \times 10^{-7}$ cm/W and $(1.1 \pm 0.5) \times 10^{-11}$ cm²/W, respectively, which are considerably greater than those of other optical materials. This large optical nonlinearity is ascribed to (a) homogeneously deposited thin nanotube film on optically transparent barium fluoride, (b) just-resonant excitation condition, and (c) intrinsic saturable absorption feature of SWNTs.

Keywords: Single wall carbon nanotube, Nonlinear absorption coefficient, Nonlinear refractive index, Z-scan technique

*Corresponding author: Tel: +81-26-269-5212; fax: +81-26-269-5208

E-mail: yak@endomoribu.shinshu-u.ac.jp

The unique one-dimensional quantum confinement of single walled carbon nanotubes (SWNTs) motivates scientists to study their optical, magnetic, and magneto-optical properties. Very recently, intensive studies on the nonlinear optical properties of SWNTs have been carried out theoretically¹ and experimentally.²⁻⁴ It is believed that SWNTs can be used in the fabrication of optical limiting and switching devices due to their nonlinear optical properties upon absorption⁴⁻⁶ and its fast decay time of less than 1 picoseconds.^{2, 7-9} These nonlinear properties are related to the third-order nonlinear susceptibility $\chi^{(3)}$, which is considered to be a complex quantity:¹⁰

$$\chi^{(3)} = \chi_R^{(3)} + i\chi_I^{(3)}. \quad (1)$$

The imaginary part is related to the nonlinear absorption coefficient β through

$$\chi_I^{(3)} = \frac{2n_0^2 \epsilon_0 c^2}{3\omega} \beta, \quad (2)$$

and the real part is expressed in terms of the nonlinear refractive index n_2 through

$$\chi_R^{(3)} = \frac{4n_0^2 \epsilon_0 c}{3} n_2, \quad (3)$$

where n_0 is the linear refractive index, ϵ_0 the dielectric permittivity of free space, c the speed of light in vacuum, and ω the laser radiation frequency.

Unfortunately, previously published studies about nonlinear optical properties of carbon nanotubes have been carried out in solution¹¹ or on poorly dispersed nanotube films and composite.² The use of nanotube suspensions results in poorly resolved data, because a large background signal inevitably exists and an inhomogeneously deposited film and dispersed composite make the absorption and reflection measurements in the same sample difficult. These drawbacks could lead to a misunderstanding of the intrinsic optical properties of SWNTs.

In the present study, well-dispersed homogeneous nanotube films exhibiting an optimized thickness were prepared by spraying nanotube solution on optically transparent substrates. We measured both the nonlinear transmission and reflection characteristics of the same sample using the Z-scan technique. The Z-scan method has great advantages because of its simplicity as well as high sensitivity, by which one can

investigate nonlinear absorption and nonlinear refraction separately.¹⁰⁻¹³ It was found that the nonlinear absorption coefficient β ($(5.4 \pm 2.0) \times 10^{-7}$ cm/W) and nonlinear refractive index n_2 ($(1.1 \pm 0.5) \times 10^{-11}$ cm²/W) measured from our homogeneously deposited SWNT films are larger or somewhat smaller than the previous values of SWNTs, and are considerably greater than those of other optical materials.

Highly purified SWNTs grown by the HiPco method were purchased from the CNL (USA). They were used without further purification. In order to prepare a uniform thin film of nanotube, we first dispersed the nanotubes in ethanol with the help of homogenizer (Kubota UP50H). By spraying the nanotube suspension onto various substrates (using an atomizer), we were able to prepare homogeneously dispersed nanotube film with a thickness of 4.2×10^{-5} cm on a transparent BaF₂ crystal (see the inset of Fig. 1 (a)). We used field-emission scanning electron microscopy (FE-SEM; JEOL JSM6335Fs) to obtain information on the morphological differences of SWNTs on different substrates. Judging from Fig. 1 (a) and Fig. 1 (b), it should be noticed that SWNTs are well dispersed to form thin and homogeneous film on a BaF₂ crystal plate in comparison with a quartz plate that showed flocculated nanotubes and uncovered surface, even though both samples were prepared under the same conditions. It is believed that the hydrophobic nature of BaF₂ attracts the hydrophobic surface of SWNTs, resulting in homogeneous deposition of thin SWNT film without large flocculation.

The nonlinear optical properties of SWNT films were examined by the open aperture Z-scan method. The excitation light source was a regenerative amplified Ti:sapphire laser (Clark-MXR, Inc. CPA-2001S) with a repetition rate of 1 kHz. The 200-fs laser pulses at a wavelength of 1.46 μ m were divided into two beams by a mirror. One weak beam was detected by a PbS photoconductive detector (D1) as reference light. The other strong beam was focused on the prepared thin SWNT films by a 10-cm focal length lens. The beam size at the focal plane was approximately 5.0×10^{-3} cm. The nanotube film sample was moved along the laser propagation direction. The transmitted and reflected light intensities were measured as a function of the sample

position z relative to the focal plane by another PbS detector (D2) in the transmission and reflection Z-scan experiments, respectively. The output of D2 was transferred to a digital oscilloscope in which it was compared with the signal of D1 in order to avoid the influence of instability of laser radiation parameters.

Optical absorption measurements on our sample were made with use of an infrared-visible spectrometer (Shimadzu, Solidspec-3700). As shown in Fig. 3, three broad absorption bands at 1.18, 1.34, and 1.44 μm correspond to the lowest E_{11}^S bands of semiconducting SWNTs. These tube diameters are estimated to be 0.95 - 1.00 nm, 0.90 - 1.09 nm, and 1.13 - 1.36 nm, respectively, on the basis of the Kataura-plot.¹⁴ In addition, the enhanced radial breathing mode (RBM) at 185 cm^{-1} (see the inset in Fig. 2) indicates the presence of the semiconducting SWNTs with diameter of 1.3 nm, because Raman frequency of RBM is inversely related to the diameter of carbon nanotubes.¹⁵ Therefore, our Z-scan experiments with the laser wavelength of 1.46 μm were just-resonant with the semiconducting SWNTs having diameter of 1.3 nm. It is noteworthy that we measured both the nonlinear transmission and reflection characteristics in the same sample prepared on BaF₂ substrate.

The result of the transmission Z-scan measurement is shown in Fig. 3 (a), where black circles indicate experimental data and solid line is the best-fitted curve described below. The Z-scan signal exhibits a maximum of transmittance at the focal point ($z = 0$), with a symmetrical shape. We did not observe any changes in the Z scan trace during the 3-h long experiment. This fact indicates good photochemical stability of SWNT films on barium fluoride. The transmission Z-scan signal is fitted by the well-established formula:¹²

$$T(Z) = 1 + \frac{\beta I_0 l}{1 + \left(\frac{z}{z_0}\right)^2}. \quad (4)$$

Here $z_0 = k\omega_0^2/2$, with the beam waist radius ω_0 at the focal point ($\approx 5.0 \times 10^{-3}$ cm) and the wave number $k = 2\pi/\lambda$; $\lambda = 1.46 \times 10^{-4}$ cm. The sample thickness l was estimated to be 4.2×10^{-5} cm from the relation $l = (2.3/\alpha_0)\log(I_{T0}/I_T)$, where α_0 is the linear

absorption coefficient ($= 6.5 \times 10^4 \text{ cm}^{-1}$ ⁷) and $\log(I_{T0}/I_T)$ means the optical density ($= 1.2$). The laser power density I_0 was about 1.5 MW/cm^2 . The theoretical fitting is in good agreement with the experimental data. From this fitting, the nonlinear absorption coefficient β was obtained as $(5.4 \pm 2.0) \times 10^{-7} \text{ cm/W}$. The main source of uncertainty in the obtained value is the absolute measurement of the laser irradiance at the focal plane.

The reflection Z-scan data is presented in Fig. 3 (b), where the solid line refers to the theoretically fitted curve using the following equation:¹³

$$R(Z) = 1 + \frac{R_0}{R_N} \frac{n_2 I_0}{1 + \left(\frac{z}{z_0}\right)^2}. \quad (5)$$

Here, $R_0 = (n_0 + ik_0 - 1)/(n_0 + ik_0 + 1)$ is the linear reflection coefficient and $R_N = \partial R/\partial n = 2/(n_0 + ik_0 + 1)^2$, with the linear refractive index $n_0 (= 2.0$ ¹⁶) and the extinction coefficient $k_0 = \alpha_0/2k$. The laser power density I_0 was about 3.5 MW/cm^2 in this case. In Fig. 3 (b), we see a symmetric bell shaped reflection with a maximum at the focal point. From the fitting of Eq. (5) to the data, the nonlinear refractive index n_2 can be estimated to be $(1.1 \pm 0.5) \times 10^{-11} \text{ cm}^2/\text{W}$.

By using Eq. (2) and Eq. (3), we obtain $\chi_I^{(3)} = 8.0 \times 10^{-9} \text{ esu}$ and $\chi_R^{(3)} = 1.4 \times 10^{-8} \text{ esu}$ from the above values of β and n_2 , respectively. These values are summarized in the upper part of Table 1, and compared with the corresponding values of SWNTs obtained previously by other groups. Our values of β and n_2 (or $\chi_I^{(3)}$ and $\chi_R^{(3)}$) are greater than those of SWNT/Triton X100 suspension¹¹ and SWNT/polyvinyl alcohol composite,² but are somewhat smaller than those of SWNT film^{7,17} and SWNT/SDS suspension¹⁸. One reason for these discrepancies might be connected to the fact that many experimental parameters are needed to evaluate the values of β and n_2 .

In order to differentiate the nonlinear optical properties of our SWNT film, we summarize the nonlinear optical parameters of various optical materials in the lower

part of Table 1. The β value of our SWNT thin film is about two orders of magnitude greater than those of CaF_2 and BaF_2 crystals,¹⁹ which have been widely used as optical windows and achromatic lenses. Our value of β is also large compared with those obtained for multi-walled carbon nanotube (MWNT) films,⁶ silicon nanocrystals,¹² and CdS thin films,²⁰ except for C_{60} films⁵. Furthermore, the present n_2 value displays about two orders of magnitude greater than that of MWNT films. In other words, the third-order nonlinear susceptibility $\chi^{(3)}$ is nicely high in our SWNT thin films. This large optical nonlinearity could be due to the homogeneously deposited thin nanotube film on optically transparent barium fluoride substrate and the just-resonance with the lowest E_{11}^S transition of semiconducting SWNTs, in addition to the intrinsic saturable absorption feature of carbon nanotubes. The surface-enhanced effect may also contribute to the growth of $\chi^{(3)}$, as in the case of C_{60} thin films⁵.

In summary, we have studied the nonlinear optical characteristics of SWNT film using open aperture Z-scan technique. The well-prepared thin film on barium fluoride substrate enables us to measure both the nonlinear absorption and reflection characteristics in the same sample. The nonlinear absorption coefficient and nonlinear refractive index are estimated to be $(5.4 \pm 2.0) \times 10^{-7}$ cm/W and $(1.1 \pm 0.5) \times 10^{-11}$ cm²/W, respectively. These values are comparable to those of other SWNT samples and much larger than those of conventional optical materials, although there are only a few exceptions. The present experiment strongly suggests that the homogeneously deposited SWNT thin films are quite suitable for application to fast switching devices using a large optical nonlinearity.

Acknowledgments

This work was supported by the CLUSTER (the second stage) of the Ministry of Education, Culture, Sports, Science, and Technology of Japan. One of the authors (M. T.) is deeply grateful for the CONACYT-México grants: 56787 (Laboratory for Nanoscience and Nanotechnology Research-LINAN) and 58899 (Inter-American Collaboration). We are also indebted to Dr. F. Kobayashi for his technical assistance in the experiments and to the Gene Research Center, Shinshu University, for providing us

its facilities.

References

1. O.E. Alon, V. Averbukh, N. Moiseyev, *Phys. Rev. Lett.* **85**, 5218 (2000).
2. Y.C. Chen, N.R. Raravikar, L.S. Schadler, P.M. Ajayan, Y.P. Zhao, T.M. Lu, G.C. Wang, X.C. Zhang, *Appl. Phys. Lett.* **81**, 975 (2002).
3. L. Liu, S. Zhang, Y. Qin, Z-X. Guo, C. Ye, D. Zhu, *Synth. Met.* **135**, 853 (2003).
4. Y. Sakakibara, S. Tatsuura, H. Kataura, M. Tokumoto, Y. Achiba, *Jpn. J. Appl. Phys.* **42**, L494 (2003).
5. R.A. Ganeev, A.I. Ryasnyansky, V.I. Redkorechev, K. Fostiropoulos, G. Priebe, T. Usmanov, *Opt. Commun.* **225**, 131 (2003).
6. H.I. Elim, W. Ji, G.H. Ma, K.Y. Lim, C.H. Sow, C.H.A. Huan, *Appl. Phys. Lett.* **85**, 1799 (2004).
7. S. Tatsuura, M. Furuki, Y. Sato, I. Iwasa, M. Tian, H. Mitsu, *Adv. Mater.* **15**, 534 (2003).
8. J-S. Lauret, C. Voisin, G. Cassabois, C. Delalande, Ph. Roussignol, O. Jost, L. Capes, *Phys. Rev. Lett.* **90**, 057404 (2003).
9. G.N. Ostojic, S. Zaric, J. Kono, M.S. Strano, V.C. Moore, R.H. Hauge, R.E. Smalley, *Phys. Rev. Lett.* **92**, 117402 (2004).
10. M. Sheik-Bahae, A.A. Said, T.H. Wei, D.J. Hagan, E.W. Van Stryland, *IEEE J. Quantum Electron.*, **26**, 760 (1990).
11. L. Vivien, E. Anglaret, D. Riehl, F. Hache, F. Bacou, M. Andrieux, F. Lafonta, C. Journet, C. Goze, M. Brunet, P. Bernier, *Opt. Commun.* **174**, 271 (2000).
12. G.V. Prakash, M. Cazzanelli, Z. Gaburro, L. Pavesi and F. Iacona, G. Franzò, F. Priolo, *J. Appl. Phys.*, **91**, 4607 (2002).
13. D.V. Petrov, *J. Opt. Soc. Am. B* **13**, 1491 (1996).
14. H. Kataura, Y. Kumazawa, Y. Maniwa, I. Umezu, S. Suzuki, Y. Ohtsuka, Y. Achiba, *Synth. Met.* **103**, 2555 (1999).
15. A. Jorio, M.A. Pimenta, A.G. Souza Filho, R. Saito, G. Dresselhaus, M.S. Dresselhaus, *New J. Phys.* **5** (2003) 139.
16. M.F. Lin, K.W.K. Shung, *Phys. Rev. B* **50**, 17744 (1994).
17. A. Maeda, S. Matsumoto, H. Kishida, T. Takenobu, Y. Iwasa, M. Shiraishi, M. Ata,

- H. Okamoto, *Phys. Rev. Lett.* **94**, 047404 (2005).
18. N. Kamaraju, S. Kumar, A.K. Sood, S. Guha, S. Krishnamurthy, C.N.R. Rao, *App. Phys. Lett.* **91**, 251103 (2007).
 19. T. Tsujibayashi, K. Toyoda, S. Sakuragi, M. Kamada, M. Itoh, *Appl. Phys. Lett.*, **80**, 2883 (2002).
 20. J. He, W. Ji, G.H. Ma, S.H. Tang, H.I. Elim, W.X. Sun, Z.H. Zhang, W.S. Chin, *J. Appl. Phys.* **95**, 6381 (2004).

Table I. Comparison of the nonlinear optical characteristics of SWNTs and various optical materials.

Samples	β (cm/W)	$\chi_1^{(3)}$ (esu)	n_2 (cm ² /W)	$\chi_R^{(3)}$ (esu)	Ref.
SWNT film (HiPco tube)	5.4×10^{-7}	8.0×10^{-9}	1.1×10^{-11}	1.4×10^{-8}	Present study
SWNT/Triton X100 suspension (Arc-discharge tube)	5.0×10^{-8}	—	1.0×10^{-12}	—	11
SWNT/polyvinyl alcohol composite (HiPco tube, pump-probe method)	—	$\approx 10^{-10}$	—	—	2
SWNT film (HiPco tube)	—	8.5×10^{-8}	—	—	7
SWNT film (HiPco tube)	—	1.5×10^{-7}	—	—	17
SWNT/SDS* suspension	1.4×10^{-6}	—	5.5×10^{-11}	—	18
MWNT film	2.9×10^{-8}	1.6×10^{-11}	3.0×10^{-13}	1.7×10^{-11}	6
C ₆₀ film	1.7×10^{-5}	1.1×10^{-8}	2.0×10^{-9}	4.8×10^{-8}	5
Silicon nanocrystals	2.0×10^{-8}	3.0×10^{-9}	—	3.8×10^{-9}	12
CdS thin film	1.0×10^{-7}	—	—	—	20
CaF ₂ crystal (Two-photon absorption)	2.0×10^{-9}	—	—	—	19
BaF ₂ crystal (Two-photon absorption)	3.0×10^{-9}	—	—	—	

* SDS indicates sodium dodecyl sulfate.

Figure Captions

Figure 1 FE-SEM images of SWNT films prepared on BaF₂ substrate (a) and on quartz substrate (b). The inset of (a) is a photograph of SWNT film on BaF₂ substrate.

Figure 2 Optical absorption spectrum of SWNT thin film. The inset shows resonant Raman spectrum obtained by 532 nm laser excitation.

Figure 3 Normalized Z-scan transmittance (a) and reflection (b) of SWNT thin film on BaF₂ substrate measured at a wavelength of 1.46 μm. The solid lines are the best-fitted curves.

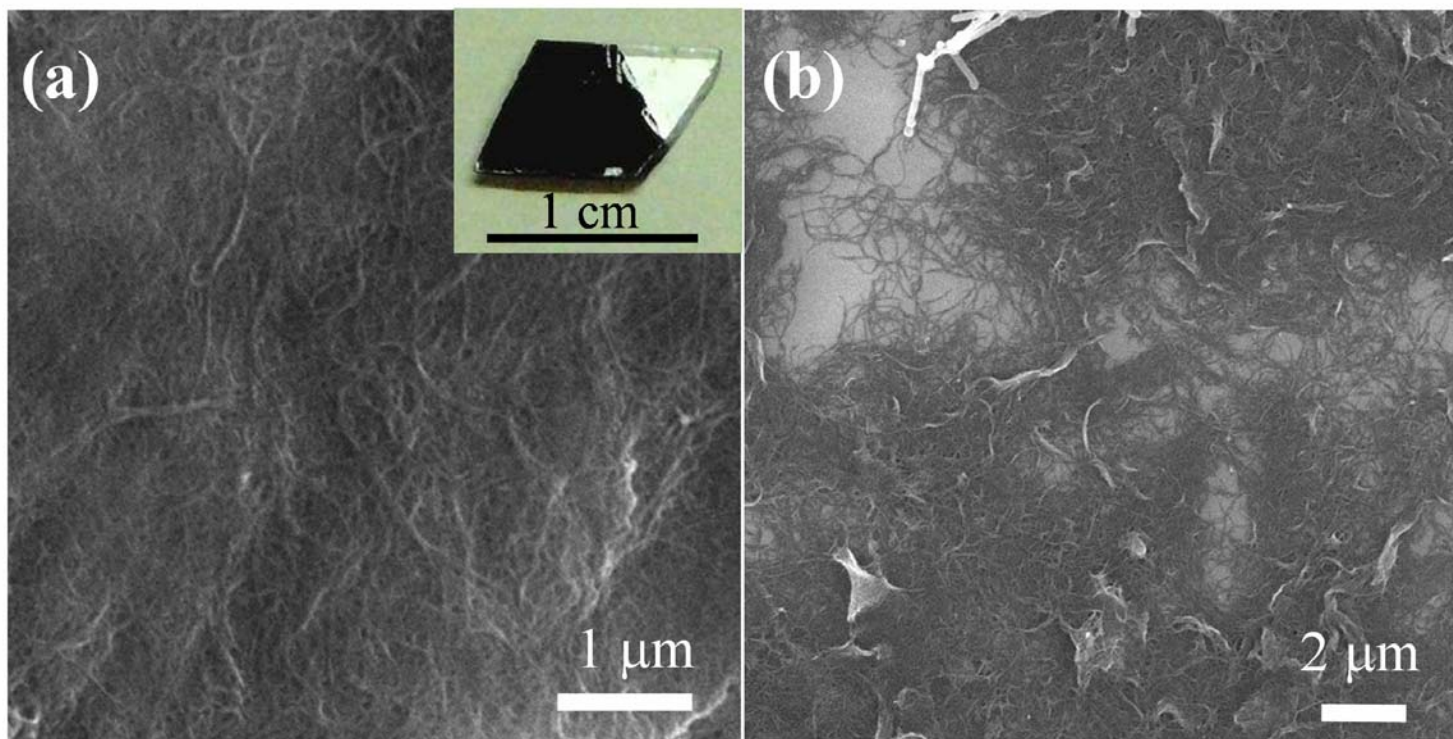


Figure 1

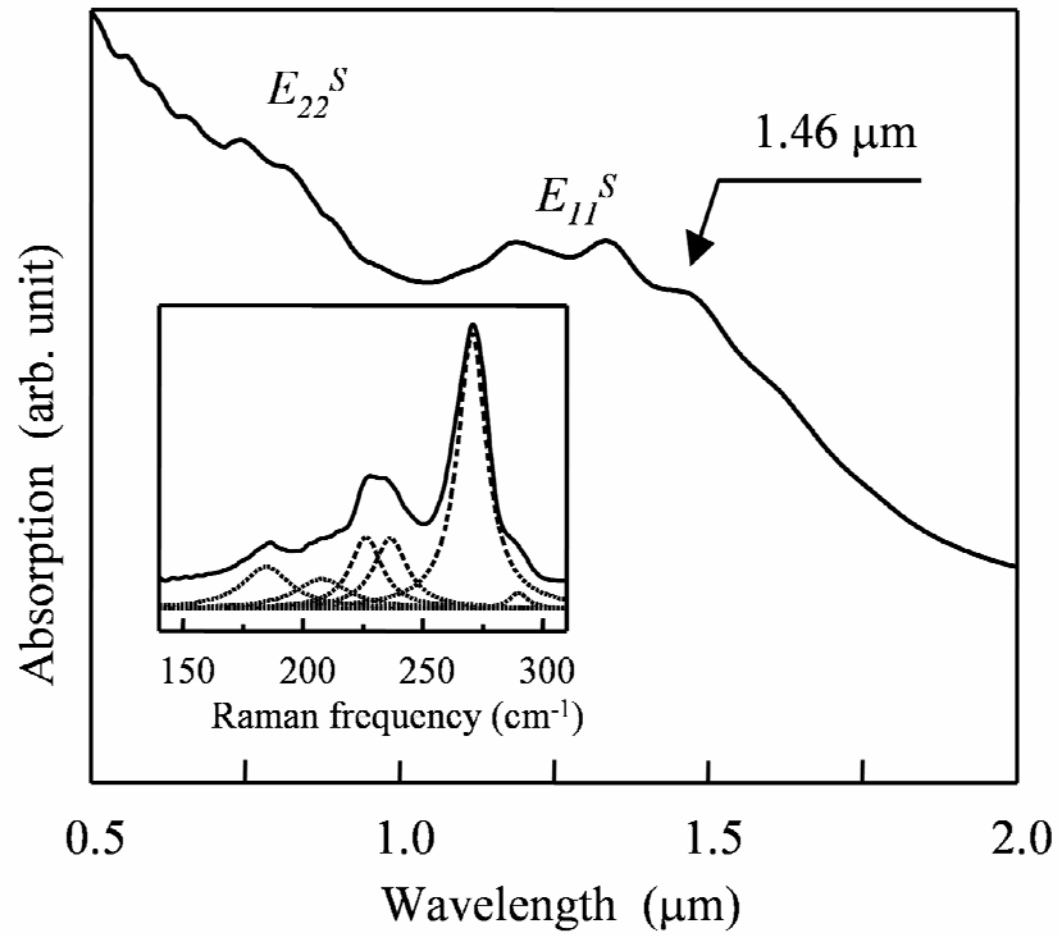


Figure 2

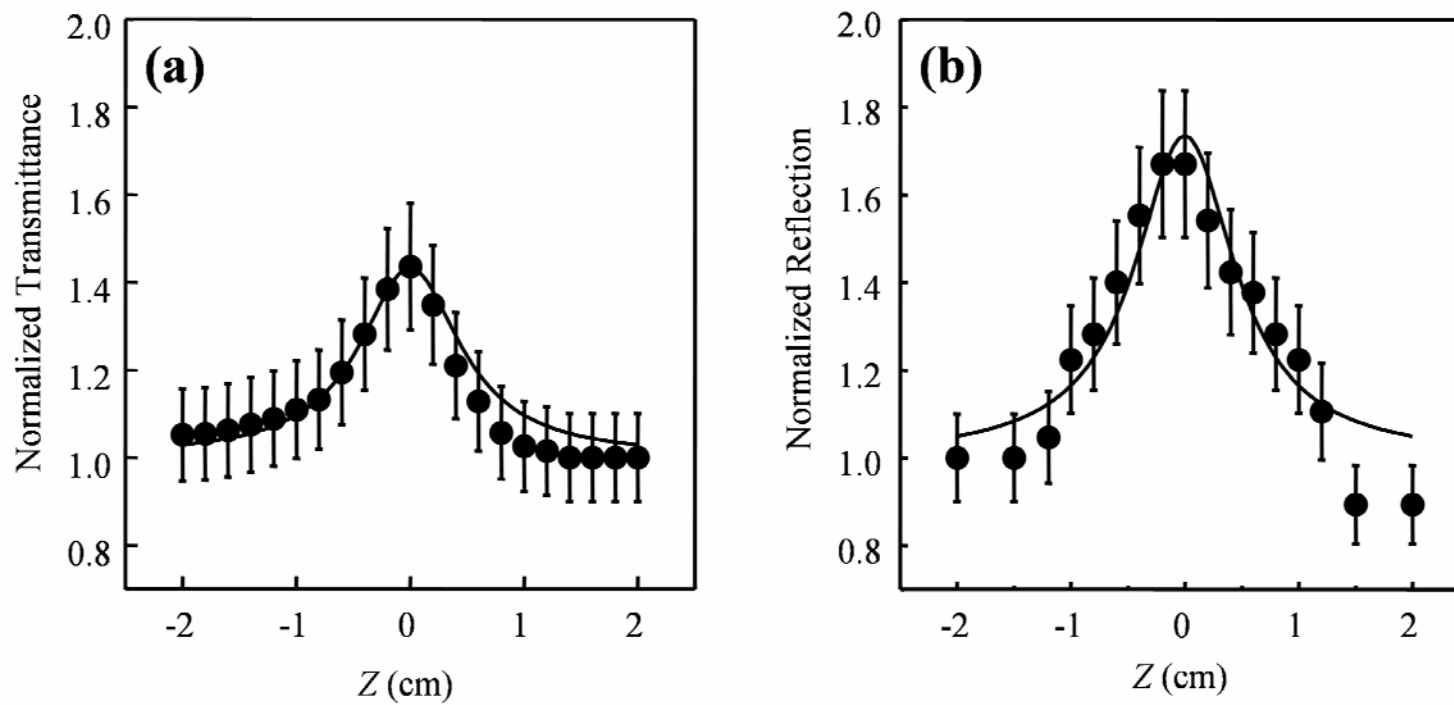


Figure 3